

1 **Revisiting the biological pump using the new continuous vertical sequestration approach**

2 Florian Ricour^{1,2*}, Lionel Guidi², Marion Gehlen³, Timothy DeVries⁴ and Louis Legendre^{2*}

3

4 ¹Sorbonne University, CNRS, Laboratoire d'Océanographie de Villefranche, LOV, F-06230
5 Villefranche-sur-Mer, France.

6 ²Freshwater and OCeanic science Unit of reSearch (FOCUS), University of Liège, Liège, Bel-
7 gium.

8 ³LSCE-IPSL, CEA, CNRS, Université Paris-Saclay, Gif-sur-Yvette, France.

9 ⁴Department of Geography / ERI / IGPMS, University of California, Santa Barbara, CA,
10 USA.

11 *Corresponding authors: florian.ricour@uliege.be and legendre@imev-mer.fr

12

13 **Running title: Continuous vertical sequestration approach**

14

15 **The ocean contains about 40 times more carbon than the atmosphere, i.e. it stores**
16 **38,000 Pg C of dissolved inorganic carbon (DIC) vs. 900 Pg C of carbon dioxide (CO₂) in**
17 **the present atmosphere. The biological carbon pump contributes to ocean carbon**
18 **storage by moving DIC out of the surface ocean into deeper waters. Many studies have**
19 **assumed that storage of biogenic DIC (DIC_{bio}) on climate-relevant timescales (typically**
20 **≥100 years) only occurs in the deep ocean. Here we show, in contrast, that this storage**
21 **can occur at all depths in the water column, mostly above 2,000 and even 1,000 m. To**
22 **illustrate this continuous vertical sequestration, we use the fraction of water that**
23 **remains in the ocean interior for ≥100 years, computed with a data-assimilated inverse**
24 **circulation model, to estimate the DIC_{bio} sequestration fluxes resulting from the**
25 **combined action of different biological pump pathways. With this new approach, global**
26 **carbon sequestration for ≥100 years driven by the biological pump is 0.9–2.6 Pg C y⁻¹,**
27 **which is up to 6 times larger than usual estimates that ignore the contribution of upper-**
28 **ocean sequestration.**

29 The biological carbon pump is an important process of natural carbon sequestration in the
30 ocean^{1,2}. Photosynthesis in sunlit surface waters converts dissolved inorganic carbon (DIC) to
31 organic carbon, and gravitational settling, ocean mixing and animal migrations export this
32 organic matter downwards where its remineralization (respiration) produces biogenic DIC
33 (DIC_{bio}; also called C_{soft}³ and C_{seq}¹). However, not all of this DIC_{bio} is sequestered on
34 climatically relevant timescales, since much is remineralized in the upper ocean where CO₂
35 can be returned to the atmosphere relatively quickly^{4–6}. Although the timescale of
36 “climatically significant” carbon storage (i.e. sequestration) does not have a strict definition⁷,
37 it is conventionally considered to be ≥100 years⁸. This 100-year time horizon has been used as
38 a guideline to assess carbon sequestration by the biological pump^{9,10}, to distinguish between
39 regions of efficient and inefficient carbon sequestration^{11,12}, and to define durable carbon
40 sequestration in assessments of the efficacy of ocean-based deliberate carbon dioxide removal
41 (CDR) approaches¹³. In the ocean sequestration literature, some studies address the inventory
42 of sequestered carbon^{1,5}, and others the sequestration flux². The present work deals with the
43 latter. Ocean carbon sequestration is detailed in Supplementary Information 1, and the
44 acronyms and symbols used in the text are listed in Supplementary Table S1.

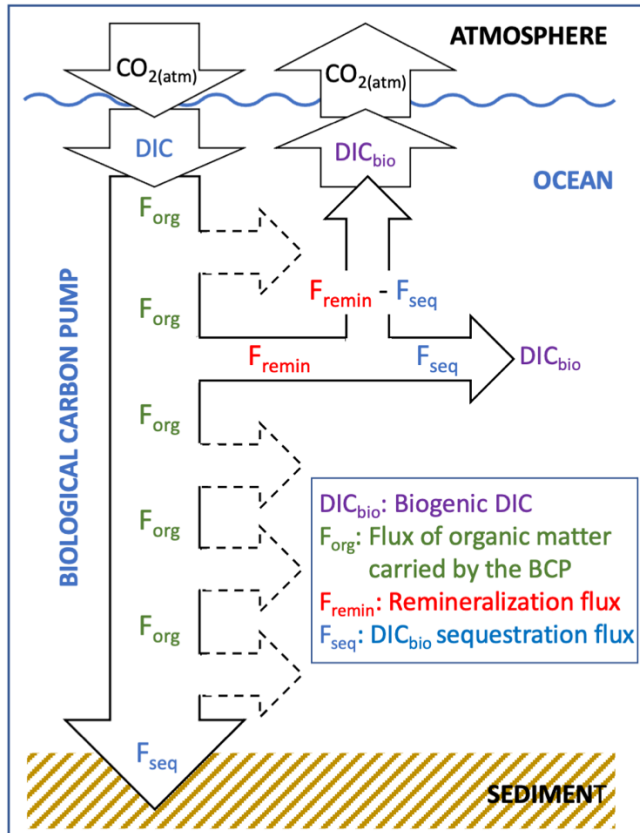
45 Despite the widespread use of the 100-year time threshold, few studies have explicitly
46 quantified the flux of carbon sequestered by the biological pump for ≥100 years, due to
47 difficulties in assessing how long DIC_{bio} will be retained in the ocean. In order to estimate the

48 biological pump sequestration flux, most previous studies have assumed that carbon
49 transported below a fixed depth or isopycnal surface – generally located between 1,000 and
50 2,000 m^{2,11,14–19} – is stored for long enough to be considered “sequestered”. An implicit
51 assumption of these studies is that DIC_{bio} above this “sequestration depth” does not remain in
52 the ocean for ≥100 years.

53 A modelling study using Lagrangian tracking found that only about 70% of the biogenic
54 carbon flux at 1000 m was sequestered for >100 years in the North Atlantic⁶. Similar
55 calculations using a global ocean circulation inverse model found that carbon injected as CO₂
56 at different ocean depths and locations showed large geographic variations in the amounts
57 retained for ≥100 years in the ocean interior⁵. For example, only about 20% of the carbon
58 injected at a depth of 1,000 m in the western North Atlantic was retained for ≥100 years,
59 while the corresponding value for injection at a similar depth in the Northeast Pacific was
60 nearly 80%. However, no study has yet assessed on the global scale how much of the carbon
61 flux driven by the biological pump is sequestered for ≥100 years.

62 Here, we use published values of the fraction of a water parcel at a given location and depth
63 that will remain in the ocean for ≥100 years (f_{100}), calculated⁵ using a data-assimilated ocean
64 circulation inverse model²⁰ to determine the fraction of DIC_{bio} sequestered in the ocean
65 interior for ≥100 years. We combine f_{100} with estimates of carbon fluxes by different
66 biological pump pathways to compute how much carbon is sequestered for ≥100 years under
67 various assumptions. To emphasize the point that sequestration for ≥100 years can occur at
68 any depth in the water column, we refer to our approach as Continuous Vertical Sequestration
69 (CONVERSE; Fig. 1). In this study, we compare the CONVERSE results with estimates
70 based on fixed depth horizons. This approach is relevant to open-ocean CDR deployments,
71 which are intended to induce large-scale export fluxes to sequester atmospheric carbon as
72 DIC in the water column.

Continuous vertical sequestration by the BCP



73

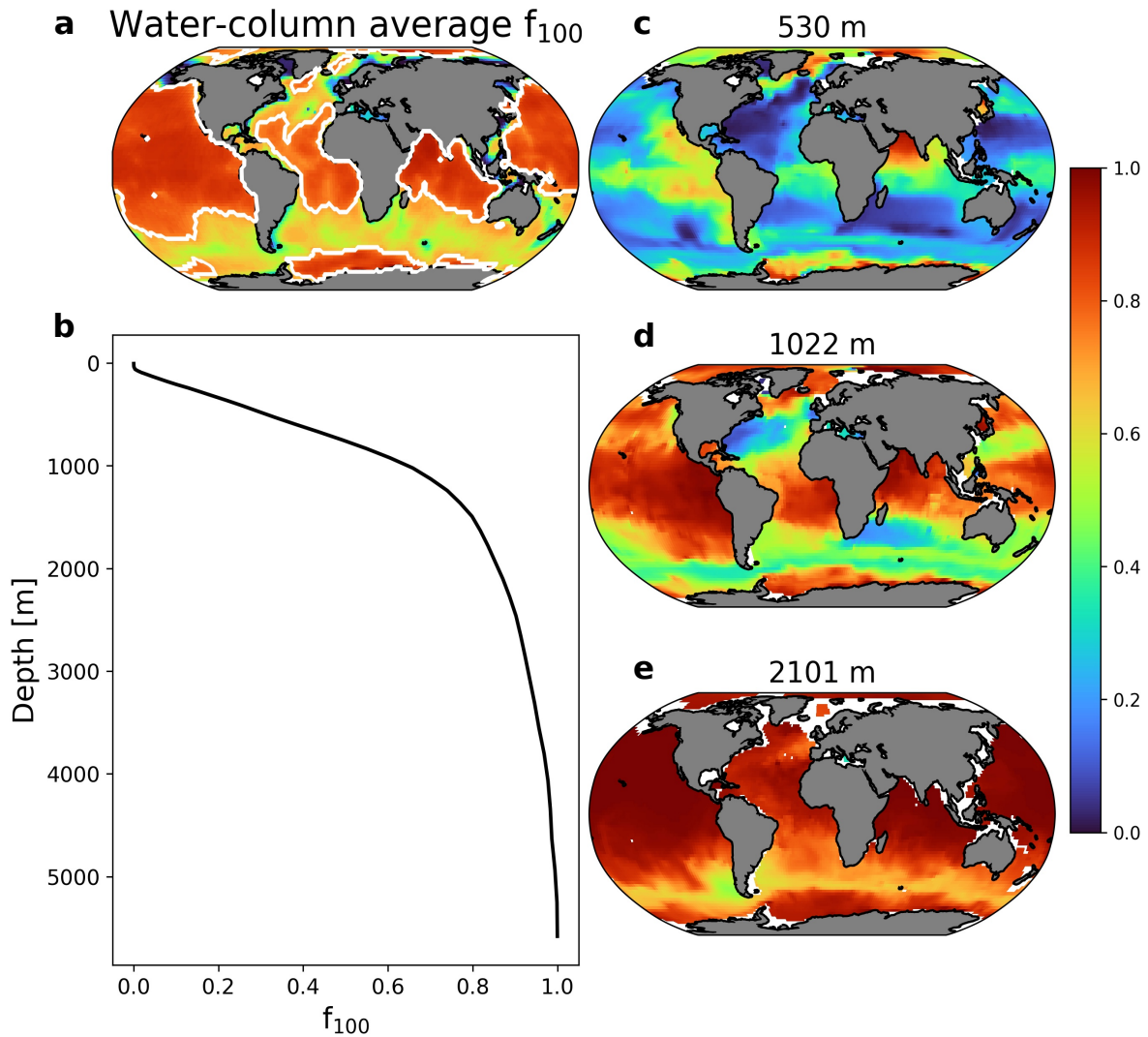
74 Fig. 1. The CONVERSE fluxes driven by the biological pump. Throughout the water column,
 75 part of the downward flux of organic carbon (F_{org}) is remineralized to CO_2 (F_{remin}). Some of
 76 the resulting DIC_{bio} returns to the atmosphere within 100 years, and the remainder is
 77 sequestered for ≥ 100 years (F_{seq}). The fraction sequestered increases with depth, but is not
 78 null even at relatively shallow depths (Fig. 2), causing continuous vertical sequestration of
 79 DIC_{bio} . In addition, a very small fraction of F_{org} (which "overflows" the biological pump) is
 80 not remineralized to DIC_{bio} at the bottom of the water column, and may be sequestered in
 81 sediment for long times reaching millions of years. The CONVERSE processes occur at all
 82 depths, but are illustrated here at only one depth, while their occurrences at some other depths
 83 are represented by dashed arrows. The widths of arrows do not reflect the magnitudes of
 84 fluxes.

85 Fraction of biogenic DIC sequestered at different depths and locations in the ocean

86 Across the ocean, there is large geographic variability in the fraction of DIC_{bio} that can be
 87 sequestered for ≥ 100 years. The median depth-average value of f_{100} is roughly 0.7, a value
 88 which can be used to separate regions with relatively lower and higher DIC_{bio} sequestration
 89 potential (Fig. 2a). The depth distribution of globally averaged f_{100} increases rapidly from 0 at
 90 the sea surface (by definition) to ~ 0.6 at 1,000 m, quite rapidly from 1,000 m to 2,000 m, and
 91 progressively up to 1.0 at the seafloor where 1.0 indicates 100% retention of DIC_{bio} for
 92 ≥ 100 years (Fig. 2b).

93 The geographic distribution of f_{100} at different depths shows that the areas occupied by higher
 94 f_{100} increase with water depth (Fig. 2c-d, and Supplementary Fig. S1). However, many areas
 95 of relatively shallow depths have high f_{100} values, with f_{100} exceeding 0.5 at 530 m in regions

such as the North Indian Ocean, Eastern Pacific, and Antarctic margin (Fig. 2c). Sequestration occurring in these regions would be missed by traditional metrics that consider sequestration to occur only below 1,000 or 2,000 m. In contrast, there are significant areas of the ocean at 1,000 m depth where f_{100} values are as low as 0.2-0.3 (Fig. 2d), and some deep waters with relatively large areas where $f_{100} < 1.0$, e.g. at 2101 m and deeper in most of the Antarctic Circumpolar Current (Fig. 2e).



102

103 Fig. 2. Geographic and vertical distributions of f_{100} : (a) depth-averaged values of f_{100} below
104 the base of the euphotic zone (z_{eu}); continuous white lines: median value of 0.7; (b) ocean-
105 averaged vertical profile of f_{100} ; (c-e) f_{100} values at three depths. White areas correspond to
106 pixels with water depths shallower than the depth illustrated (more depths in Supplementary
107 Fig. S1).

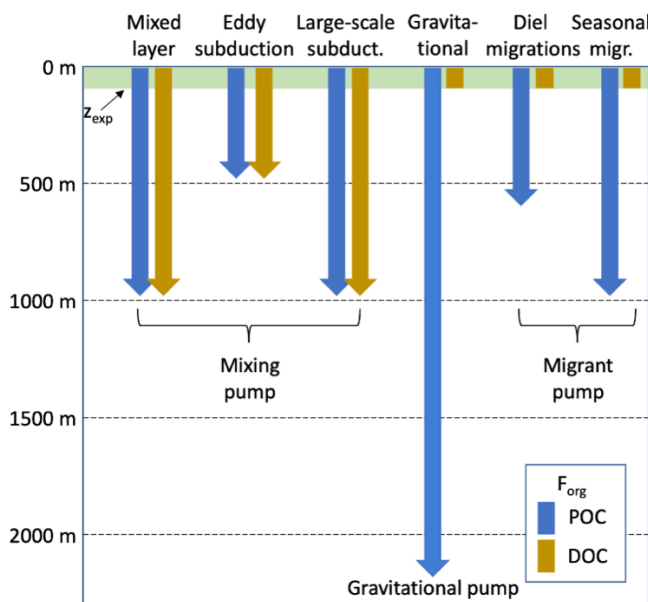
108 The results in Fig. 2 highlight important points regarding biological pump-driven carbon
109 sequestration. First, not all water at depths $\geq 1,000$ or $\geq 2,000$ m is stored away from the
110 atmosphere (and thus the carbon it contains sequestered) for ≥ 100 years, contrary to the tacit
111 assumption of studies that use a fixed depth horizon for assessing sequestration fluxes.
112 Second, sequestration in the form of DIC_{bio} can occur throughout the entire water column.
113 The global-ocean depth-averaged f_{100} for depths $> 1,000$ m is 0.87, indicating that most, but
114 not all, of the water in the deep sea is stored away from the atmosphere with the carbon it

115 contains for ≥ 100 years. However, the more important point from Fig. 2 is that a substantial
116 fraction of the water above 1,000 m is also stored away from the atmosphere for ≥ 100 years,
117 thus sequestering the carbon it contains, for example at 530 and 319 m where the global
118 average f_{100} is 0.33 and 0.18, respectively.

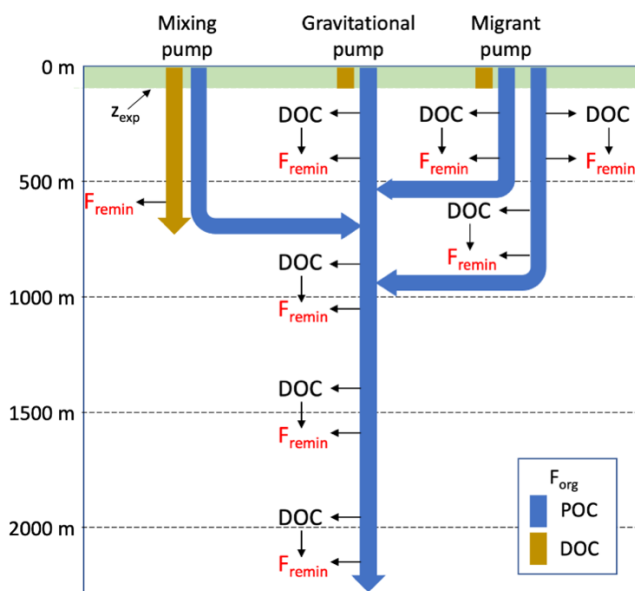
Mechanisms of biological-pump carbon transport and remineralization profiles

119 In order to assess the carbon sequestered by the biological pump for ≥ 100 years, we combined
120 our estimates of f_{100} with estimates of carbon fluxes due to the biological pump. The latter
121 operates by three distinct mechanisms or “pathways” which all contribute to carbon
122 sequestration¹ (details in Supplementary Information 2). The *gravitational pump* is driven by
123 the sinking of particulate organic carbon (POC), consisting mostly of phytoplankton cells and
124 aggregates²¹ and zooplankton faecal pellets and debris²². Some of the sinking POC reaches
125 the seafloor, although most is remineralized in the water column²³. The physical *mixing pump*
126 is driven by the seasonal shoaling and deepening of the mixed layer²⁴, the subduction of water
127 masses and their organic carbon along mesoscale to sub-mesoscale fronts associated with
128 eddies^{25,26} and the large-scale advection and overturning of the ocean²⁷⁻²⁹. The mixing pump
129 mechanisms transport surface water downwards with its POC and dissolved organic carbon
130 (DOC). The *migrant pump* is composed of animals that perform diel or seasonal vertical
131 migrations^{30,31}. During these migrations, animals defecate, excrete DOC and release
132 respiratory CO₂ deep in the water column, the source of this carbon being POC grazed in
133 upper waters. Migrating animals also release some biogenic carbon at various depths during
134 their vertical journeys.

a Maximum depths of POC and DOC vertical BCP fluxes



b Organic matter remineralization by the combined pumps



135

136 Fig. 3. The biological carbon pump. (a) Maximum depths to which each mechanism
 137 transports POC and DOC below the export depth (z_{exp}), and the carbon pump to which each
 138 belongs. (b) Combined action of the three pumps on F_{remin} : one part of the POC flux is
 139 remineralized directly, and another part is solubilized to DOC by bacteria or released as DOC
 140 by grazers, after which most of this DOC is remineralized. There are reports of zooplankton
 141 seasonal vertical migrations deeper than 1000 m.

142 Each of these pathways has a characteristic depth above which the exported carbon is
 143 remineralized to CO_2 in the water column (Fig. 3a; values from Table 2 of a published
 144 paper³²), this depth determining how much of the resulting DIC_{bio} can be sequestered for ≥ 100
 145 years. The deepest depth is reached by the gravitational pump, which can potentially transport
 146 POC all the way to the seafloor. The POC carried by the other pumps that is not remineralized
 147 above the depths they reach is incorporated into the gravitational pump for the remainder of
 148 its journey downwards (Fig. 3b). Most of the carbon exported by the mixing pump, which is

149 the only pump that carries DOC, is remineralized to CO₂ in the upper 1000 m, except in areas
150 of deep convection where labile DOC can be found ≥ 1000 m³³. A small fraction of labile
151 DOC is converted into refractory DOC, thus sequestering carbon chemically^{17,34,35}, but this
152 “microbial pump” is beyond the scope of the present study. In the migrant pump, vertically
153 migrating animals remineralize at depth carbon transported in their bodies. The depth of diel
154 migrations generally does not exceed 200 m, but can reach a maximum of 600 m in some
155 cases^{36,37} while seasonal migrants can reach 1400 m³⁸ and even deeper^{39–41}.

156 For each of these pumps, we estimated the flux sequestered for ≥ 100 years (F_{seq}) by
157 calculating the three-dimensional remineralization rate of carbon in the interior ocean and
158 multiplying it by the corresponding value of f_{100} (see Methods). We refer to the global integral
159 of this quantity as the global sequestration flux. We define the interior ocean as all depths
160 below a fixed “export depth”, which we choose as 100 m or the base of the euphotic zone,
161 depending on our model configuration (Table 1). Although it is theoretically possible for
162 sequestration to occur above this depth horizon due to non-zero values of f_{100} at relatively
163 shallow depths (Fig. 2 and Supplementary Fig. S1), for purposes of this study we assumed
164 that sequestration above the export depth is negligible. We computed F_{seq} using seven
165 different CONVERSE versions, whose characteristics are summarized in Table 1 and
166 Supplementary Table S2. We use various published estimates of carbon export and
167 remineralization fluxes (F_{remin}) driven by the gravitational, mixing and migrant pumps. We
168 compare the CONVERSE F_{seq} to estimates at fixed depth horizons of 1,000 and 2,000 m
169 (Table 1) and also to previously published values^{14,15,18} (Supplementary Table S3).

Table 1. *Upper part.* Estimates of biological pump fluxes for the seven CONVERSE versions (C1 to C7): export depth; characteristics of calculations of F_{remin} for POC, DOC, vertical migrations and sediment. We multiplied F_{remin} by the corresponding f_{100} to calculate F_{seq} . *Lower part.* Values of global-ocean CONVERSE F_{seq} (Pg C y^{-1}) and percent ratios (%) over the water column by the gravitational and all pumps, and also calculated at 1000 and 2,000 m and above and below 2000 m; values normalized to the corresponding export flux at 100 m. Ratios of CONVERSE F_{seq} to POC fluxes calculated at 1,000 and 2,000 m. Equations and detailed values are given in Supplementary Tables S2 to S5. The global distributions of F_{seq} in C1, C2 and C4 are illustrated in Fig. 5.

CONVERSE	1	2	3	4	5	6	7
Export depth	100 m	100 m	100 m	z_{eu}	100 m	100 m	100 m
Pump or flux	Computation of pixel remineralization fluxes (F_{remin}) (Pg C m⁻² y⁻¹)						
Gravitational*	$b = 0.86$	Variable b	Regional b	C4-C5: Taken from a model ⁴	Based on C5 [†]	Same as C1	
Mixing		C1-C3: based on C5 [†]		C4-C5: Taken from a model ⁴	Based on C5 [†]	Based on POC export at 100 m	
Migrant diel			C1-C7: Derived from POC export at 100 m				
Migrant seasonal[‡]	C1-C3: Derived from POC flux at 597 m		C4-C5: Derived from POC flux at 619 m		Based on C5 [†]	Same as C1	
Sediment	C1-C7: Published global-ocean estimates of fluxes in the sediment ⁴²						
Pumps	Global water-column sequestration fluxes (F_{seq}) and % ratios						
Gravitational*	0.63	0.92	0.71	1.89	1.86	0.76	0.63
Biological (all)*	0.88	1.16	0.95	2.61	2.44	1.00	0.96
Gravitational* /all	72%	79%	75%	72%	76%	76%	66%
Mixing+migrant / all	28%	21%	25%	28%	24%	24%	34%
Fluxes	Global fluxes calculated at 1,000 and 2,000 m (F_{seq})						
POC at 1,000 m[§]	0.38	0.68	0.47	1.13	1.13	0.46	0.38
POC at 2,000 m[§]	0.19	0.42	0.26	0.47	0.47	0.19	0.19
Pumps	Global sequestration fluxes integrated above and below 2,000 m (F_{seq}) and % ratios						
Gravitational $\leq 2,000$ m	0.48	0.54	0.49	1.61	1.58	0.64	0.48
Gravitational $> 2,000$ m*	0.15	0.38	0.22	0.28	0.28	0.12	0.15
All $\leq 2,000$ m	0.71	0.77	0.71	2.30	2.13	0.87	0.81
All $> 2,000$ m*	0.17	0.39	0.24	0.31	0.31	0.13	0.15
All_{≤2000} / All_{owc}^{**}	81%	66%	75%	88%	87%	87%	84%
All_{>2000} / All_{owc}^{**}	19%	33%	25%	12%	11%	13%	16%
Pumps or fluxes	Global sequestration fluxes normalized to POC export fluxes at 100 m (F_{seq}^*)^{††}						
Gravitational*	0.21	0.31	0.24	0.22	0.25	0.25	0.21
Biological (all)*	0.29	0.39	0.32	0.30	0.33	0.33	0.32
POC at 1,000 m[§]	0.13	0.23	0.16	0.13	0.15	0.15	0.13
POC at 2,000 m[§]	0.06	0.14	0.09	0.05	0.06	0.06	0.06
Pump ratios	CONVERSE sequestration fluxes to POC fluxes at 1,000 and 2,000 m						
• to POC flux at 1,000 m							
Gravitational*	1.7	1.4	1.5	1.7	1.6	1.7	1.7
Biological*	2.3	1.7	2.0	2.3	2.2	2.2	2.5
• to POC flux at 2,000 m							
Gravitational*	3.3	2.2	2.7	4.0	4.0	4.0	3.3
Biological (all)*	4.6	2.8	3.7	5.6	5.2	5.3	5.1

* Water column only, i.e. does not include F_{seq} in sediment

† Value from C5 multiplied by the ratio of the global POC export flux at 100 m of C1 to C5

‡ Northern North Atlantic only

§ Calculated at 1,000 or 2000 m, assuming that the POC flux at 1,000 or 2,000 m is entirely sequestered below

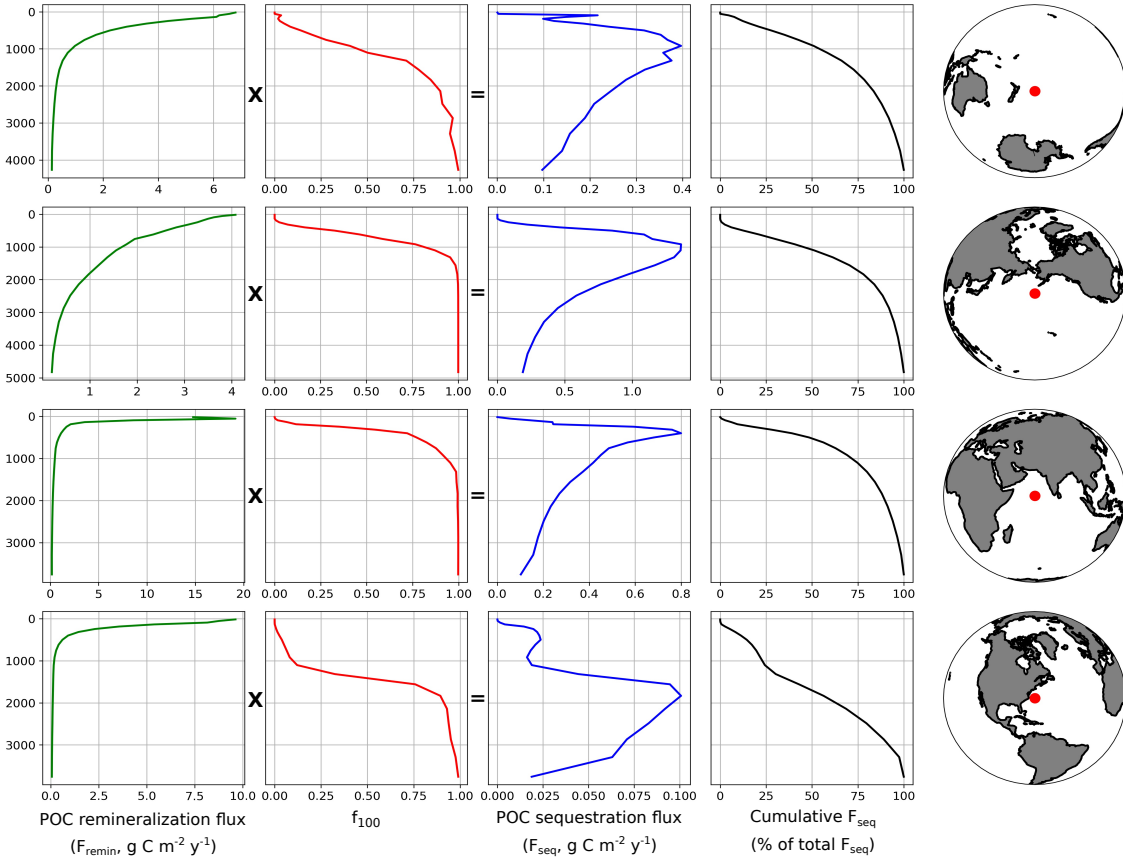
** All_{owc}: F_{seq} for all pumps over the water column

†† $F_{seq}^*(\text{global}) = F_{seq}(\text{global})/F_{exp}(\text{global})$, where F_{exp} is the POC flux at the export depth (Supplementary Tables S3-S5)

170 Estimates of sequestration fluxes by the biological pump

171 For calculating carbon sequestration by the gravitational pump, we use two approaches. The
172 first combines estimates of carbon export at 100 m from a model¹⁵ with an empirical power-
173 law relationship governing the attenuation of particle flux with depth⁴³ to determine F_{remin} .
174 The coefficient of POC attenuation with depth (b) in this model is varied in our different

175 calculations using a globally uniform $b = 0.86^{43}$, a geographically variable b from an
 176 empirical model¹⁵, and a regionalized b in biogeochemical provinces¹⁸. The second approach
 177 uses model output (SIMPLE-TRIM) from a data-assimilated biological pump model⁴ to
 178 determine F_{remin} , with an export depth of either 100 m or the base of the euphotic zone.
 179 Carbon export at 100 m from these models is illustrated in Supplementary Fig. S2.



180

181 Fig. 4. Vertical profiles of F_{remin} (Supplementary eq. 24), f_{100} , and the resulting F_{seq} (eq. 6) for
 182 POC and cumulative F_{seq} from surface to depth, in four ocean pixels representative of
 183 different ocean configurations identified in the present study. The vertical profiles of F_{remin} are
 184 calculated with data from SIMPLE-TRIM⁴. The values of F_{remin} and F_{seq} (X-axes) are different
 185 for the four sites.

186 The vertical profiles of POC F_{seq} , resulting from the combination of vertical profiles of F_{remin}
 187 and f_{100} , generally showed maxima above 2,000 and even 1,000 m and at least 50% of vertical
 188 F_{seq} accumulation by 1,000 m (Fig. 4). This shows that the time-honored use of 2,000 m or
 189 1,000 m as sequestration depth misses most of the ocean sequestration flux, and thus stresses
 190 the significance of the CONVERSE approach. The location of F_{seq} maxima between 1,000
 191 and 2,000 m reflects the relatively high values of both f_{100} and F_{remin} at these depths, whereas
 192 studies that estimate F_{seq} at 1,000 or 2,000 m^{2,11,14-19} only consider sequestration below these
 193 depths where f_{100} is high but very little POC is left to be remineralized.

194 The results in Fig. 4 explain why the sequestration flux of POC due to the gravitational pump
 195 estimated by the CONVERSE approach is 0.63-1.89 Pg C y⁻¹, depending on the set of
 196 parameters used in the calculations, while the corresponding sinking POC flux calculated at
 197 2,000 m is only 0.19-0.47 Pg C y⁻¹ (Table 1). The fraction of the global POC export flux by
 198 the gravitational pump at 100 m that is sequestered for ≥ 100 years (F_{seq}^*) is 0.21-0.31, which

199 is up to 2 and 4 times greater than the fraction of the carbon export flux that reaches 1,000 and
200 2000 m, respectively (Table 1). Similarly, F_{seq}^* of previous studies underestimate the
201 corresponding CONVERSE F_{seq}^* by a factor of 1.8-3.0 when the gravitational pump global
202 POC was estimated at 2,000 m^{14,15}, and by a factor of 1.3 when it was estimated at the top of
203 the permanent pycnocline¹⁸ (Supplementary Table S3).

204 Our F_{seq}^* calculated at 1,000 m can be compared to the particle transfer efficiency used in
205 some studies to quantify the fraction of the POC exported at 100 m that bypasses
206 remineralization above 1,000 m, although these studies did not consider possible
207 sequestration of DIC_{bio} above 1,000 m^{11,16,19}. Our F_{seq}^* at 1,000 m (0.13-0.23; Table 1) are
208 consistent with published average regional transfer efficiencies to 1,000 m ranging between
209 <0.05 and 0.25^{11,19}.

210 In our calculations, F_{seq} by the biological pump (all components together) ranges from 0.88 to
211 2.61 Pg C y^{-1} (Table 1). This wide range largely results from the wide range of carbon export
212 values used in our calculations (3.0-8.6 Pg C $year^{-1}$, Supplementary Tables S3 and S4), and
213 also the wide methodological differences among the seven CONVERSE versions. When
214 considering F_{seq}^* (i.e. the fraction of the carbon export flux included in F_{seq}), the much
215 narrower range of 0.29-0.39 (Table 1) indicates that this fraction is less variable.

216 While the gravitational pump accounts for 66-79% of the carbon sequestration flux by the
217 biological pump (Table 1), the mixing and migrant pumps contribute together the remaining
218 21-34%, which is substantial. Using F_{seq} for DOC (by the mixing pump) and a combination of
219 model-based estimates and correlations with POC export (migrant pump) (see Methods), we
220 estimate that the two pumps represent 11-23 and 9-12%, respectively, of the global
221 sequestration driven by the biological pump (the role of the migrant pump is underestimated
222 because we only have flux estimates for the northern North Atlantic) (Supplementary
223 Tables S3 and S4; Supplementary Information 3 provides comparisons with values from the
224 literature).

225 When adding the mixing and migrant pumps to the CONVERSE framework, we estimate that
226 global F_{seq}^* is 0.29-0.39, an increase of 0.08 relative to the sole gravitational pump, and 2-3 or
227 3-6 times higher than the global F_{seq}^* of 0.13-0.23 and 0.05-0.14 when considering only the
228 POC flux at 1,000 or 2,000 m, respectively (Table 1). Similarly, previous studies cited above
229 underestimated biological pump global F_{seq}^* by a factor of 1.8-4.0 relative to the CONVERSE
230 calculations (Supplementary Table S3). This reinforces our above finding that the POC flux
231 estimated at either 1,000 and 2000 m significantly underestimates the sequestration efficiency
232 of the biological pump. Global F_{seq} in sediment represents a small additional sequestration
233 flux, corresponding to 0.3-1% of global POC export and 1-3% of the global water-column
234 sequestration flux (Supplementary Tables S3 and S4).

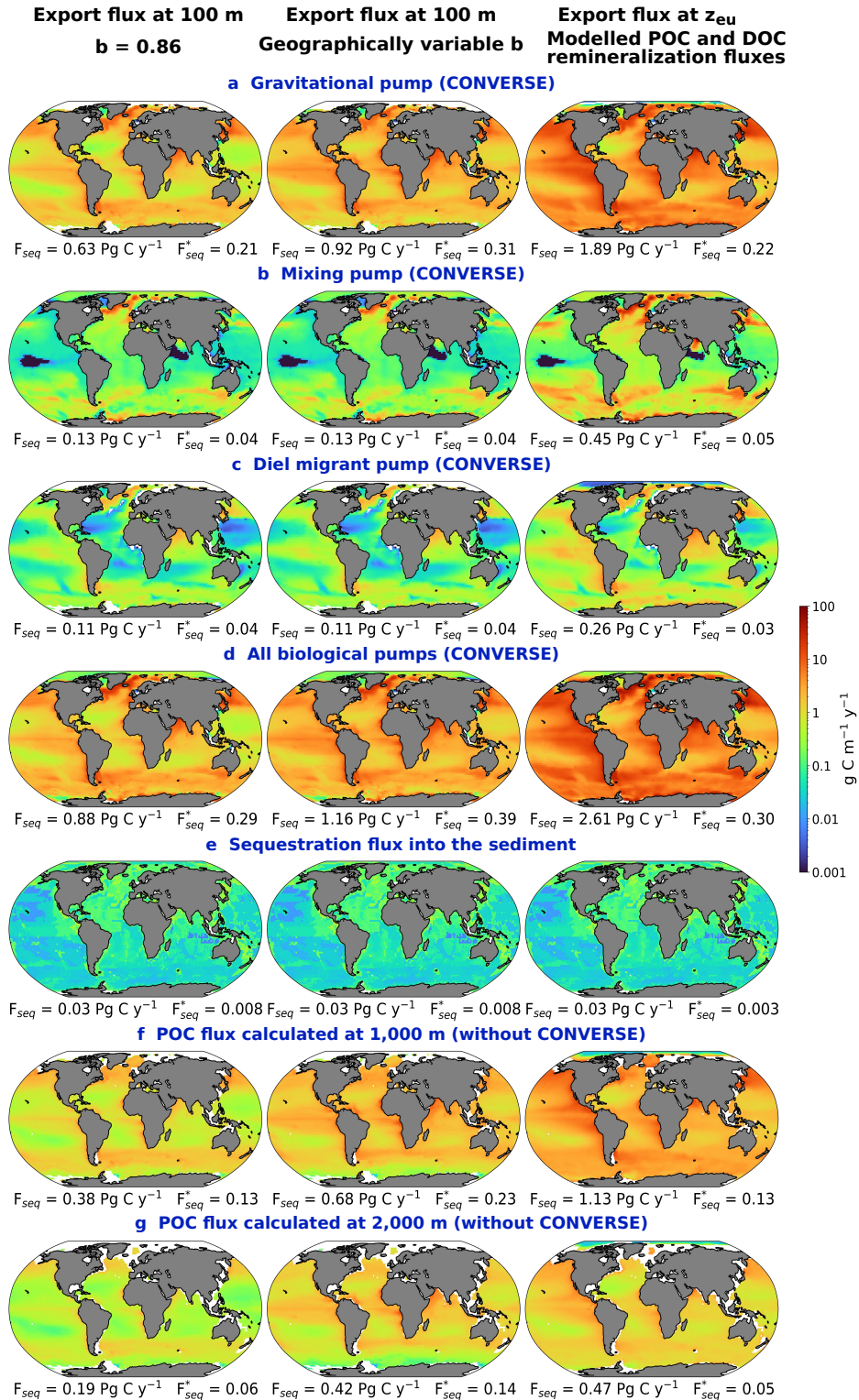
235 Sequestration above and below 2,000 m accounts for 66-88% and 11-33%, respectively, of
236 the global flux (Table 1). Corresponding values for 1,000 m are 47-68% and 32-53%,
237 respectively (Supplementary Table S5). The sequestration flux below 2,000 m is slightly
238 lower than the sinking POC flux at 2,000 m (0.15-0.38 and 0.19-0.47 Pg C y^{-1} , respectively)
239 because some of the DIC_{bio} in waters >2000 m is not stored there for ≥ 100 years, a point also
240 made by other authors⁶. However, this DIC_{bio} loss is more than compensated by the
241 sequestration of DIC_{bio} above 2,000 m (0.48-1.61 Pg C y^{-1}). Thus, neglecting sequestration
242 above 2,000 m results in significant underestimation of global F_{seq} .

243 The geographic distributions of carbon sequestration fluxes by the three pumps and the whole
244 biological pump, illustrated for three representative CONVERSE versions in Fig. 5 (all
245 versions in Supplementary Figs. S3 and S4), are similar among versions and provide insights
246 into the environmental controls of sequestration. The global distribution of F_{seq} by the whole
247 biological pump mainly reflects that of the gravitational pump (Fig. 5a,d). Sequestration by
248 the biological and gravitational pumps is low in subtropical gyres where export and f_{100}
249 <1,000 m are both low, and high in equatorial and subarctic waters and the Antarctic
250 Circumpolar Current where POC export and/or $f_{100} < 1,000$ m are high (Fig. 2 and
251 Supplementary Figs. S1 and S2). This is also the case of the diel migrant pump and the POC
252 flux calculated at 1,000 and 2,000 m. Values of F_{seq} by the mixing pump generally reflect
253 those of POC export. The distributions of the POC flux calculated at 1,000 and 2,000 m are
254 qualitatively similar to those of the CONVERSE biological and gravitational pump, but
255 quantitatively much lower consistent with the above global F_{seq} values.

256 Discussion

257 The main finding of our study is that remineralization of carbon transported by the biological
258 pump can sequester carbon (as DIC_{bio}) not only in deep waters but throughout the water
259 column. This is contrary to previous studies that assessed the sequestration flux of the
260 biological pump by measuring or computing carbon flux at a given depth horizon, as deep as
261 2,000 m. These studies calculated the sequestration flux as if it only occurred below the given
262 depth, and did not include sequestration in the upper and mid-water column as if DIC_{bio} above
263 the sequestration depth was rapidly lost to the atmosphere. In the CONVERSE framework,
264 our calculations show significant DIC_{bio} sequestration fluxes (i.e. storage for ≥ 100 years) over
265 most of the water column (Fig. 4), and much greater carbon sequestration driven by
266 remineralization above 2,000 m than below (Table 1). Furthermore, the migration and mixing
267 pumps contribute at least 21-34% of the sequestration flux by the biological pump (Table 1)
268 even though they do not transport carbon into the deep ocean. These pumps are ignored by
269 most traditional metrics of carbon sequestration.

270 Our calculations show that the carbon sequestration flux by the whole biological pump is 2-3
271 or 3-6 times larger than usually estimated based on POC fluxes at 1,000 or 2,000 m,
272 respectively, and the CONVERSE sequestration flux estimates are up to 4 times larger than
273 those from previously published studies. Biogeochemical models should thus compute F_{seq}
274 over all water-column depths. We suggest that F_{seq} be implemented in the model experiments
275 used to evaluate future CDR options⁴⁴, with the required f_{100} values computed with available
276 equations¹. The f_{100} values could instead be the same as the published values¹ used in this
277 study, which may however be affected by changes in ocean circulation due to climate change
278 and variability. In evaluations of future ocean CDR strategies, biologically-driven carbon
279 sequestration fluxes should also be estimated over the whole water column.”



280

281 Fig. 5. Biogenic carbon F_{seq} in CONVERSE 1, 2 and 4: (a-d) carbon pumps; (e) F_{seq} into the
 282 sediment, and the POC flux calculated at (f) 1,000 m and (g) 2000 m. The latter two are the
 283 total sequestration fluxes estimated in many studies. The seasonal migrant pump is not
 284 illustrated because our results concern the sole northern North Atlantic. Ocean areas shallower
 285 than 100 m are without colour.

286 **Methods**287 ***Calculation of F_{seq}^****

288 We calculated the fraction of the global POC export flux by the gravitational pump at 100 m
 289 that is sequestered for more than 100 years as a ratio of fluxes. This generated a
 290 dimensionless quantity:

291 $F_{\text{seq}}^*(\text{global}) = F_{\text{seq}}(\text{global})/F_{\text{exp}}(\text{global})$ (1)

292 where F_{exp} is the POC flux at the export depth $z_{\text{exp}} = 100$ m.

293 ***Estimation of the fraction of sequestered biogenic CO₂ at different depths and locations in***
 294 ***the global ocean***

295 The fraction of water at different depths and locations that does not come back to the ocean
 296 surface (upper 10 m) within 100 years (f_{100} ; called $f(t)$ in another publication⁵) is a
 297 dimensionless quantity ranging from 0.0 at surface to 1.0 at bottom although the deepest
 298 calculated f_{100} may be <1.0 in some pixels (2° longitude x 2° latitude). We generated f_{100} for
 299 48 discrete depths (z') from 5 m down to the maximum value of 5582 m in each pixel of the
 300 global ocean with water depth ≥ 5 m, i.e. all $f_{100}(<5 \text{ m}) = 0.0$. The f_{100} values are available at
 301 <https://doi.org/10.6084/m9.figshare.15228690.v2> However as explained in the text, we did
 302 not use the $f_{100} < z_{\text{eu}}$.

303 For further calculations, we considered that each $f_{100}(z')$ was representative of a depth interval
 304 Δz ranging from depth z [mid-point between the depth above z' (i.e. $z'-1$) and z'] to $(z+1)$
 305 [mid-point between z' and the depth below z' (i.e. $z'+1$)]. Hence:

306 $\Delta z = (z+1) - z = [(z' + 1) - (z' - 1)] / 2$ (2)

307 where the dimensions of z , z' and Δz were [L]. The shallowest Δz ranged from below z_{eu} to
 308 the next calculable z . The deepest Δz ranged from the deepest calculable z [mid-point between
 309 the deepest z' and z' above] to the deepest z' .

310 The correspondence between f_{100} values for each depth z' and depth interval Δz was as
 311 follows:

312 $f_{100}(z') = f_{100}(\Delta z)$ (3)

313 We calculated the weighted depth-averaged fraction of biogenic CO₂ sequestered over the
 314 whole water column below z_{eu} as follows:

315 $f_{100}(\text{pixel}) = \sum_{\Delta z=\text{shallowest}}^{\text{deepest}} \left[f_{100}(\Delta z) \times \left(\frac{\Delta z}{\sum_{\Delta z=\text{shallowest}}^{\text{deepest}} \Delta z} \right) \right]$ (4)

316 where Δz were the successive depth intervals from below z_{eu} to depth, and $\left(\frac{\Delta z}{\sum_{\Delta z=\text{shallowest}}^{\text{deepest}} \Delta z} \right)$
 317 were the weights.

318 ***Continuous vertical approach to the estimation of sequestration fluxes***

319 We used three different data sources for our calculations of seven different CONVERSE
 320 versions. The first was an empirical model of POC F_{seq} (F_{seqPOC}) in the global ocean¹⁵. Using
 321 these data, we computed 1-D (vertical) downward fluxes. The second source was a numerical

322 3-D circulation-biological pump model⁴, whose data were available at
323 <https://tdevries.erl.ucsb.edu/models-and-data-products/> under the SIMPLE-TRIM output. We
324 used the concentrations and remineralization rates of different fractions of POC and DOC at
325 various depths to compute POC and DOC F_{remin} . The third source was a global synthesis of
326 sediment composition and burial flux⁴², which provided values of the flux of organic carbon
327 in the sediment (F_{seqSed}). The data sources we used for the different CONVERSE versions are
328 identified in Supplementary Table S2, and input POC F_{exp} values are illustrated in
329 Supplementary Fig. S2. We estimated sequestration by the different pumps only in the pixels
330 where water depth was >100 m.

331 In addition, the second dataset⁴ contained 12 versions of the data we used for our calculations.
332 The authors ran their model separately for each of the 12 versions, after which they computed
333 mean values. We did the same for our CONVERSE calculations with these data.

334 We generally calculated the flux of organic carbon remineralized to DIC_{bio} in each depth
335 interval Δz in the water column as the difference between the downward flux of organic
336 carbon $F_{\text{org}}(z)$ at two successive depths z and $(z + 1)$:

$$337 F_{\text{remin}}(\Delta z) = F_{\text{org}}(z) - F_{\text{org}}(z + 1) \quad (5)$$

338 where all fluxes (F) had dimensions [$\text{M L}^{-2} \text{T}^{-1}$], and the masses were in units of carbon. In
339 eq. 5, we assumed that the decrease in F_{org} between depths z and $(z + 1)$ caused an equivalent
340 increase in F_{remin} , i.e. the remineralization biogenic carbon produced an equivalent flux of
341 DIC_{bio} . The Δz could differ among biological pumps depending on the data used in the
342 calculations.

343 We then computed the sequestration flux of DIC_{bio} in Δz by multiplying $F_{\text{remin}}(\Delta z)$ by the
344 corresponding $f_{100}(\Delta z)$ value (eq. 3):

$$345 F_{\text{seq}}(\Delta z) = F_{\text{remin}}(\Delta z) \times f_{100}(\Delta z) \quad (6)$$

346 Calculations corresponding to eq. 6 are illustrated for POC in Fig. 4. We obtained local F_{seq} in
347 each pixel with water depth >100 m by summing up the $F_{\text{seq}}(\Delta z)$ over all depth intervals in the
348 pixel:

$$349 \text{Pixel } F_{\text{seq}} = \sum_{\Delta z = \text{shallowest}}^{\text{deepest}} F_{\text{seq}}(\Delta z) \quad (7)$$

350 Finally, we estimated global-ocean F_{seq} by summing up pixel F_{seq} multiplied by the pixel's
351 area over all pixels containing data:

$$352 \text{Global } F_{\text{seq}} = \sum_{\text{All pixels}} [\text{Pixel } F_{\text{seq}} \times \text{Pixel area}] \quad (8)$$

353 where the dimensions of pixel areas and $F_{\text{seq}}(\text{global})$ were [L^2] and [M T^{-1}], respectively. All
354 equations below provide estimates of fluxes in ocean pixels ($\text{g C m}^{-2} \text{y}^{-1}$).

355 ***Continuous vertical estimation of pixel sequestration fluxes in CONVERSE 1***

356 We describe here the calculations for CONVERSE 1. We provide in the *Supplementary*
357 *Methods* the differences between CONVERSE 2 to CONVERSE 7 and CONVERSE 1 or other
358 versions.

359 • **Sediment**

360 We did not include the carbon sequestration flux into the sediment in the pumps because
361 F_{seqSed} is not always considered to be part of biological-pump-driven sequestration
362 (Supplementary Information 1). However, we needed estimates of F_{seqSed} below to calculate
363 the gravitational-pump sequestration flux (eq. 12).

364 We derived F_{seqSed} from published fluxes of total organic carbon in world-ocean sediment
365 (F_{TOC} ⁴²). In the publication (their Fig. 4C), there were no pixel F_{TOC} values for areas shallower
366 than 1,000 m or without observations, and we replaced the missing data by median F_{TOC}
367 values in depth bins (Supplementary Table S6).

368 We checked that the F_{TOC} values were consistent with our calculations by comparing them to
369 the values of the sequestration flux of all pumps together (F_{seqAll} ; eq. 20) in pixels.
370 Supplementary Table S7 shows that F_{TOC} was only a small fraction of F_{seqAll} (median of all
371 pixels: 0.02). We thus assumed that:

372 $F_{\text{seqSed}} = F_{\text{TOC}}$ (9)

373 • **Gravitational pump**

374 The gravitational pump consists of the POC sinking flux below z_{exp} . For CONVERSE 1, we
375 estimated F_{seqPOC} by calculating $F_{\text{orgPOC}}(z)$ with a widely-used empirical model⁴³:

376 $F_{\text{orgPOC}}(z) = F_{\text{expPOC}} \times (z/z_{\text{exp}})^{-b}$ (10)

377 where F_{expPOC} and $F_{\text{orgPOC}}(z)$ are the downward fluxes of POC at depth $z_{\text{exp}} = 100$ m and any
378 depth z below z_{exp} , respectively, and the coefficient of POC flux attenuation with depth $b =$
379 0.86⁴³. The dimensions of F and z are [$\text{M L}^{-2} \text{T}^{-1}$] and [L], respectively, and exponent b is
380 dimensionless.

381 For all depth intervals Δz deeper than z_{exp} , we calculated $F_{\text{remInPOC}}(\Delta z)$ with eq. 5, using
382 $F_{\text{orgPOC}}(z)$ from eq. 10:

383 $F_{\text{remInPOC}}(\Delta z) = F_{\text{orgPOC}}(z) - F_{\text{orgPOC}}(z + 1)$ (11)

384 where the shallowest Δz ranged from z_{exp} to the next z below. We calculated $F_{\text{seqPOC}}(\Delta z)$ with
385 eq. 6.

386 For F_{orgPOC} remaining at the bottom of the deepest Δz , $F_{\text{orgPOC}}(\text{deepest } z')$, we considered that
387 the F_{seqSed} fraction in the pixel (eq. 9) was entirely sequestered in the sediment and the
388 remaining fraction was partly sequestered in deep waters:

389 $F_{\text{seqPOC}}(\text{deep}) = [F_{\text{orgPOC}}(\text{deepest } z') - F_{\text{seqSed}}] \times f_{100}(\text{deepest } \Delta z)$ (12)

390 Because real f_{100} below the deepest Δz may be larger than our $f_{100}(\text{deepest } \Delta z)$, it is possible
391 that eq. 12 slightly underestimated $F_{\text{seqPOC}}(\text{deep})$ in some pixels. We calculated F_{seqPOC} with
392 eq. 7.

393 • **Mixing pump**

394 We explain in the text that the estimates of F_{seqPOC} reflect the combined action of the three
395 pumps on these fluxes. (Fig. 3b). The mixing pump transports not only POC, but also DOC
396 produced above z_{exp} . The different components of this pump reach different injection depths,

397 which we combined into a single z_{mix} , and their combination creates F_{orgDOC} from z_{mix}
398 downwards.

399 A practical problem is that the data required to estimate the magnitude of $F_{\text{reminDOC}}(\Delta z)$ by
400 each of the three physical injection mechanisms of the mixing pump in all pixels of the global
401 ocean – which would be required to calculate pixel and global F_{seqDOC} – do not generally exist
402 in the literature. To get around this constraint, we computed estimates of F_{reminDOC} and F_{seqDOC}
403 for the whole mixing pump.

404 For CONVERSE 1, we used the concentrations of DOC ([DOC]; [M L⁻³]) and their
405 remineralization rates (k; [T⁻¹]) in four DOC fractions (labile, semi-labile, semi-refractory,
406 and refractory) within each depth interval Δz [L] from SIMPLE-TRIM. With these data, we
407 computed $F_{\text{reminDOC}}(\Delta z)$ as follows:

$$408 F_{\text{reminDOC}}(\Delta z) = \sum_{\text{4 fractions}} ([\text{DOC}] \times k \times \Delta z) \quad (13)$$

409 where the dimensions of [DOC], k and Δz were [M L⁻³], [T⁻¹] and [L], respectively. We
410 calculated Δz and pixel F_{seq} with eqs. 6 and 7.

411 However, the value of $F_{\text{expPOC}} = 3.0 \text{ Pg C y}^{-1}$ at $z_{\text{exp}} = 100 \text{ m}$ ¹⁵ we used in CONVERSE 1 was
412 different from the corresponding value of 7.3 Pg C y^{-1} in SIMPLE-TRIM⁴ (see also the legend
413 of Supplementary Fig. S2), and we thus multiplied the values of F_{seqDOC} derived from eqs. 13,
414 6 and 7 by the ratio of the two F_{exp} :

$$415 F_{\text{seqDOC}} = F_{\text{seqDOC}} \text{ from eqs. 13, 6 and 7} \times (3.0 \text{ Pg C y}^{-1} / 7.3 \text{ Pg C y}^{-1}) \quad (14)$$

416 The geographic distributions of the two F_{expPOC} at $z_{\text{exp}} = 100 \text{ m}$ are illustrated in
417 Supplementary Fig. S2).

418 • *Migrant pump: diel vertical migrations*

419 Diel vertical migrations by zooplankton, fish, jellies and other animals transport organic
420 matter from the upper water column downwards, where part of it is released to surrounding
421 waters as POC and DOC and is remineralized to DIC_{bio}, thus creating $F_{\text{reminMigrD}}$.

422 In all versions of CONVERSE, we assumed that remineralization occurred at the depth
423 reached by migrating animals, i.e. no remineralization of F_{expMigrD} above this depth:

$$424 F_{\text{reminMigrD}} = F_{\text{expMigrD}} \quad (15)$$

425 Modelling studies estimated that global F_{expMigrD} by zooplankton was equal to 14% of global
426 F_{expPOC} at the base of the euphotic zone³⁶, and by all migrating animals ranging in size
427 between 0.2 mm and 20 cm was 18% of global F_{expPOC} at 150 m³¹. We used these two
428 estimates as follows. On the one hand, given that the global ratio euphotic/100 m of
429 $F_{\text{expPOC}}(\text{global})$ is $8.6 \text{ Pg C y}^{-1} / 7.3 \text{ Pg C y}^{-1} = 1.2$ (corrected values, which are slightly
430 different from those in the original publication⁴), we multiplied the above 14%³⁶ by 1.2 to
431 obtain global F_{expMigrD} by zooplankton = 17% of global F_{expPOC} at 100 m. On the other hand,
432 using the above 18% of global F_{expPOC} at 150 m³¹ and eq. 10 with $b = 0.86$, we back calculated
433 global F_{expPOC} by zooplankton and other animals up to 20 cm as 25% of global F_{expPOC} at
434 100 m. We used the latter value because it included zooplankton and other migrating animals,
435 and applied it to all pixels of the global ocean:

$$436 F_{\text{reminMigrD}} = F_{\text{expMigrD}} = 0.25 F_{\text{expPOC}}, \text{ at } z_{\text{exp}} = 100 \text{ m} \quad (16)$$

437 Vertically migrating animals reach depths $z_{migrD} = 200$ to 600 m (Supplementary
438 Information 2), and we assumed for our calculations that all migrating animals reached the
439 f_{100} depth of $z_{migrD} = 320$ m (depth for which f_{100} values were available):

440 $F_{seqMigrD} = F_{reminMigrD} \times f_{100}(320 \text{ m})$ (17)

441 • *Migrant pump: seasonal vertical migrations*

442 Deep seasonal vertical migrations of zooplankton occur in different regions of the world
443 ocean, and are best documented in the northern North Atlantic. We estimated the carbon flux
444 created by these migrations in the latter region, where a study reported that the copepod
445 *Calanus finmarchicus* generated a seasonally remineralization flux (the study used the word
446 "sequestered") at $z_{migrS} = 600$ to $1,400$ m³⁸. For CONVERSE 1, we used eq. 10 to compute
447 $F_{orgPOC}(z)$:

448 $F_{reminMigrS} = F_{expPOC} \times (z_{migrS}/z_{exp})^b$ (18)

449 where $z_{migrS} = 597$ m, $z_{exp} = 100$ m, and $b = 0.86$.

450 We assumed that all migrating animals overwintered at the f_{100} depth of $z_{migrS} = 597$ m (depth
451 for which f_{100} values were available), and used eq. 6 to obtain $F_{seqMigrS}$:

452 $F_{seqMigrS} = F_{reminMigrS} \times f_{100}(597 \text{ m})$ (19)

453 We calculated $F_{seqMigrS}$ in the northern North Atlantic by adding together the fluxes from this
454 region (eq. 8).

455 • *All pumps together*

456 To obtain the sequestration fluxes of all pumps together, we combined the above estimates for
457 the four pathways for both pixels and the global ocean:

458 $F_{seqAll} = F_{seqPOC} + F_{seqDOC} + F_{seqMigrD} + F_{seqMigrS}$ (20)

459 Because our estimates of $F_{seqMigrS}$ were limited to the northern North Atlantic, our global
460 values of F_{seqAll} outside this region were slightly underestimated as were also our values of
461 F_{seqAll} .

462 The fact that F_{seqSed} was subtracted in eq. 12 and not included in eq. 20 means that our F_{seqAll}
463 estimates did not include F_{seqSed} , as explained above. If one wished to include F_{seqSed} in the
464 pumps, its values (eq. 9) could easily be added to the pixel estimates of F_{seqAll} (eq. 20) and
465 thus included in global F_{seqAll} .

466 • *Gravitational pump at 1,000 and 2000 m*

467 We calculated the POC flux at two fixed depths, $z_{fixed} = 1,000$ m and $2,000$ m, assuming that
468 the POC flux at z_{fixed} was entirely sequestered below, i.e. $f_{100} = 1.0$. We calculated the POC
469 flux at each z_{fixed} using eq. 10 with $z = z_{fixed}$, $z_{exp} = 100$ m, and $b = 0.86$.

470 • *Gravitational pump and all pumps below and above 1,000 and 2000 m*

471 We calculated F_{seqPOC} and F_{seqDOC} below and above the two z_{fixed} . Given that most vertical
472 migrations do not exceed 1,000 m (Fig. 3a), we considered that there were only two
473 sequestration fluxes below either z_{fixed} value, i.e. F_{seqPOC} and F_{seqDOC} . We used the same
474 equations for the two z_{fixed} values:

475 $F_{\text{seqAll}}(>z_{\text{fixed}}) = F_{\text{seqPOC}}(>z_{\text{fixed}}) + F_{\text{seqDOC}}(>z_{\text{fixed}})$ (21)

476 *First*, we calculated pixel $F_{\text{seqPOC}}(>z_{\text{fixed}})$ for all CONVERSE versions as we had done for the
477 whole water column, including only the depth intervals $\Delta z > z_{\text{fixed}}$. We then calculated pixel
478 $F_{\text{seqPOC}}(\leq z_{\text{fixed}})$ as follows:

479 $F_{\text{seqPOC}}(\leq z_{\text{fixed}}) = F_{\text{seqPOC}} \text{ over the water column} - F_{\text{seqPOC}}(>z_{\text{fixed}})$ (22)

480 *Second*, we calculated $F_{\text{seqDOC}}(>z_{\text{fixed}})$ as we had done for the whole water column, including
481 only the depth intervals $\Delta z > z_{\text{fixed}}$. We calculated $F_{\text{seqDOC}}(\leq z_{\text{fixed}})$ as we had done for POC
482 (eq. 22).

483 *Third*, we used eq. 21 to calculate pixel $F_{\text{seqAll}}(>z_{\text{fixed}})$, and the resulting value to calculate
484 $F_{\text{seqAll}}(\leq z_{\text{fixed}})$:

485 $F_{\text{seqAll}}(\leq z_{\text{fixed}}) = F_{\text{seqAll}} \text{ over the water column} - F_{\text{seqAll}}(>z_{\text{fixed}})$ (23)

486

- 487 **References**
- 488 1. Siegel, D. A., DeVries, T., Cetinić, I. & Bisson, K. M. Quantifying the ocean's
489 biological pump and its carbon cycle impacts on global scales. *Ann. Rev. Mar. Sci.* **15**,
490 (2022).
- 491 2. Iversen, M. H. Carbon export in the ocean: A biologist's perspective. *Ann. Rev. Mar. Sci.*
492 **15**, (2023).
- 493 3. Wilson, J. D. *et al.* The biological carbon pump in CMIP6 models: 21st century trends
494 and uncertainties. *Proc. Natl. Acad. Sci. U. S. A.* **119**, e2204369119 (2022).
- 495 4. DeVries, T. & Weber, T. The export and fate of organic matter in the ocean: New
496 constraints from combining satellite and oceanographic tracer observations. *Global*
497 *Biogeochem. Cycles* **31**, 535–555 (2017).
- 498 5. Siegel, D. A., DeVries, T., Doney, S. & Bell, T. Assessing the sequestration time scales
499 of some ocean-based carbon dioxide reduction strategies. *Environ. Res. Lett.* (2021)
500 doi:10.1088/1748-9326/ac0be0.
- 501 6. Baker, C. A., Martin, A. P., Yool, A. & Popova, E. Biological carbon pump
502 sequestration efficiency in the north Atlantic: A leaky or a long-term sink? *Global*
503 *Biogeochem. Cycles* **36**, (2022).
- 504 7. IPCC. Annex I: Glossary [Weyer, N.M. (ed.)]. In: IPCC Special Report on the Ocean
505 and Cryosphere in a Changing Climate [Pörtner, H.-O. *et al.* (eds.)], pp. 677–702
506 (Cambridge University Press, 2019).
- 507 8. Fearnside, P. M. Why a 100-Year Time Horizon should be used for Global Warming
508 Mitigation Calculations. *Mitigation and Adaptation Strategies for Global Change* **7**, 19–
509 30 (2002).
- 510 9. Lampitt, R. S. *et al.* Ocean fertilization: a potential means of geoengineering? *Philos.*
511 *Trans. A Math. Phys. Eng. Sci.* **366**, 3919–3945 (2008).
- 512 10. Passow, U. & Carlson, C. A. The biological pump in a high CO₂ world. *Mar. Ecol. Prog. Ser.* **470**, 249–272 (2012).
- 514 11. Weber, T., Cram, J. A., Leung, S. W., DeVries, T. & Deutsch, C. Deep ocean nutrients
515 imply large latitudinal variation in particle transfer efficiency. *Proc. Natl. Acad. Sci. U.*
516 *S. A.* **113**, 8606–8611 (2016).
- 517 12. Boyd, P. W., Claustre, H., Levy, M., Siegel, D. A. & Weber, T. Multi-faceted particle
518 pumps drive carbon sequestration in the ocean. *Nature* **568**, 327–335 (2019).
- 519 13. National Academies of Sciences, Engineering, and Medicine; Division on Earth and Life
520 Studies; Ocean Studies Board; Committee on A Research Strategy for Ocean-based
521 Carbon Dioxide Removal and Sequestration. *A Research Strategy for Ocean-based*
522 *Carbon Dioxide Removal and Sequestration*. (National Academies Press (US), 2022).
- 523 14. Honjo, S., Manganini, S. J., Krishfield, R. A. & Francois, R. Particulate organic carbon
524 fluxes to the ocean interior and factors controlling the biological pump: A synthesis of
525 global sediment trap programs since 1983. *Prog. Oceanogr.* **76**, 217–285 (2008).
- 526 15. Henson, S. A., Sanders, R. & Madsen, E. Global patterns in efficiency of particulate
527 organic carbon export and transfer to the deep ocean. *Global Biogeochem. Cycles* **26**,
528 (2012).
- 529 16. Robinson, J. *et al.* How deep is deep enough? Ocean iron fertilization and carbon
530 sequestration in the Southern Ocean. *Geophys. Res. Lett.* **41**, 2489–2495 (2014).
- 531 17. Legendre, L., Rivkin, R. B., Weinbauer, M. G., Guidi, L. & Uitz, J. The microbial
532 carbon pump concept: Potential biogeochemical significance in the globally changing
533 ocean. *Prog. Oceanogr.* **134**, 432–450 (2015).
- 534 18. Guidi, L. *et al.* A new look at ocean carbon remineralization for estimating deepwater
535 sequestration. *Global Biogeochem. Cycles* **29**, 1044–1059 (2015).

- 536 19. Cram, J. A. *et al.* The role of particle size, ballast, temperature, and oxygen in the
537 sinking flux to the deep sea. *Global Biogeochem. Cycles* **32**, 858–876 (2018).
- 538 20. Holzer, M., DeVries, T. & de Lavergne, C. Diffusion controls the ventilation of a Pacific
539 Shadow Zone above abyssal overturning. *Nat. Commun.* **12**, 4348 (2021).
- 540 21. Alldredge, A. L. & Gotschalk, C. C. Direct observations of the mass flocculation of
541 diatom blooms: characteristics, settling velocities and formation of diatom aggregates.
542 *Deep Sea Res. A* **36**, 159–171 (1989).
- 543 22. Turner, J. T. Zooplankton fecal pellets, marine snow, phytodetritus and the ocean's
544 biological pump. *Prog. Oceanogr.* **130**, 205–248 (2015).
- 545 23. Dunne, J. P., Sarmiento, J. L. & Gnanadesikan, A. A synthesis of global particle export
546 from the surface ocean and cycling through the ocean interior and on the seafloor.
547 *Global Biogeochem. Cycles* **21**, (2007).
- 548 24. Dall'Olmo, G., Dingle, J., Polimene, L., Brewin, R. J. W. & Claustre, H. Substantial
549 energy input to the mesopelagic ecosystem from the seasonal mixed-layer pump. *Nat.
550 Geosci.* **9**, 820–823 (2016).
- 551 25. Omand, M. M. *et al.* Eddy-driven subduction exports particulate organic carbon from the
552 spring bloom. *Science* **348**, 222–225 (2015).
- 553 26. Resplandy, L., Lévy, M. & McGillicuddy, D. J., Jr. Effects of eddy-driven subduction on
554 ocean biological carbon pump. *Global Biogeochem. Cycles* **33**, 1071–1084 (2019).
- 555 27. Hansell, D., Carlson, C., Repeta, D. & Schlitzer, R. Dissolved organic matter in the
556 ocean: A controversy stimulates new insights. *Oceanography* **22**, 202–211 (2009).
- 557 28. Liu, L. L. & Huang, R. X. The global subduction/obduction rates: Their interannual and
558 decadal variability. *J. Clim.* (2012).
- 559 29. Levy, M. *et al.* Physical pathways for carbon transfers between the surface mixed layer
560 and the ocean interior. *Global Biogeochem. Cycles* **27**, 1001–1012 (2013).
- 561 30. Bianchi, D., Stock, C., Galbraith, E. D. & Sarmiento, J. L. Diel vertical migration:
562 Ecological controls and impacts on the biological pump in a one-dimensional ocean
563 model. *Global Biogeochem. Cycles* **27**, 478–491 (2013).
- 564 31. Aumont, O., Maury, O., Lefort, S. & Bopp, L. Evaluating the potential impacts of the
565 diurnal vertical migration by marine organisms on marine biogeochemistry. *Global
566 Biogeochem. Cycles* **32**, 1622–1643 (2018).
- 567 32. Claustre, H., Legendre, L., Boyd, P. W. & Levy, M. The Oceans' Biological Carbon
568 Pumps: Framework for a Research Observational Community Approach. *Frontiers in
569 Marine Science* **8**, (2021).
- 570 33. Hansell, D. A. Recalcitrant dissolved organic carbon fractions. *Ann. Rev. Mar. Sci.* **5**,
571 421–445 (2013).
- 572 34. Jiao, N. *et al.* Microbial production of recalcitrant dissolved organic matter: long-term
573 carbon storage in the global ocean. *Nat. Rev. Microbiol.* **8**, 593–599 (2010).
- 574 35. Jiao, N. *et al.* The microbial carbon pump and the oceanic recalcitrant dissolved organic
575 matter pool. *Nat. Rev. Microbiol.* **9**, 555–555 (2011).
- 576 36. Archibald, K. M., Siegel, D. A. & Doney, S. C. Modeling the impact of zooplankton
577 Diel vertical migration on the carbon export flux of the biological pump. *Global
578 Biogeochem. Cycles* **33**, 181–199 (2019).
- 579 37. Brun, P. *et al.* Climate change has altered zooplankton-fuelled carbon export in the North
580 Atlantic. *Nat Ecol Evol* **3**, 416–423 (2019).
- 581 38. Jónasdóttir, S. H., Visser, A. W., Richardson, K. & Heath, M. R. Seasonal copepod lipid
582 pump promotes carbon sequestration in the deep North Atlantic. *Proc. Natl. Acad. Sci.
583 U. S. A.* **112**, 12122–12126 (2015).

- 584 39. Auel, H., Klages, M. & Werner, I. Respiration and lipid content of the Arctic copepod
585 Calanus hyperboreus overwintering 1 m above the seafloor at 2,300 m water depth in the
586 Fram Strait. *Mar. Biol.* **143**, 275–282 (2003).
- 587 40. Hirche, H. J., Muyakshin, S., Klages, M. & Auel, H. Aggregation of the Arctic copepod
588 Calanus hyperboreus over the ocean floor of the Greenland Sea. *Deep Sea Res. Part I* **53**,
589 310–320 (2006).
- 590 41. Visser, A. W., Grønning, J. & Jónasdóttir, S. H. Calanus hyperboreus and the lipid
591 pump. *Limnol. Oceanogr.* **62**, 1155–1165 (2017).
- 592 42. Hayes, C. T. *et al.* Global ocean sediment composition and burial flux in the deep sea.
593 *Global Biogeochem. Cycles* **35**, (2021).
- 594 43. Martin, J. H., Knauer, G. A., Karl, D. & Broenkow, W. W. VERTEX: carbon cycling in
595 the northeast Pacific. *Deep Sea Research Part A. Oceanographic Research Papers* **34**,
596 267–285 (1987).
- 597 44. Boyd, P. *et al.* Operational monitoring of open-ocean carbon dioxide removal
598 deployments: Detection, attribution, and determination of side effects. *Oceanography*
599 (2023) doi:10.5670/oceanog.2023.s1.2.
- 600

601 **Acknowledgements**

602 We thank Dr. Louis Prieur for his calculations for early versions of the manuscript and
603 numerous suggestions, and Dr. Gabriel Reygondeau for his contributions to early versions.
604 We are grateful to Prof. Stephanie Henson (Henson et al. 2012) for providing us her data of
605 POC F_{exp} , which we used to calculate sequestration fluxes in CONVERSE 1-3, 6 and 7. We
606 also thank Dr. Sigrún Huld Jónasdóttir and Prof. Andy Visser for additional information on
607 values in their 2015 paper (Jónasdóttir et al. 2015). We also thank the two reviewers for their
608 very useful comments and suggestions.

609 This work was supported by the Fonds de la Recherche Scientifique (FNRS) of Belgium
610 (F.R.). L.G and M.G have received funding from the European Union’s Horizon 2020
611 research and innovation programme under grant agreement No 862923. This output reflects
612 only the authors’ views, and the European Union cannot be held responsible for any use that
613 may be made of the information contained therein.

614 **Author contributions**

615 L.G., T.D. and L.L. conceived the initial project. F.R. and T.D. performed data curation. F.R.,
616 T.D. and L.L. conducted the modelling and analyses, and wrote the manuscript with inputs
617 from L.G. and M.G. All authors discussed and contributed intellectually to the interpretation
618 of the results.

619 **Competing financial interests**

620 The authors declare no competing financial interests.

621 **Additional information**

622 Supplementary information for this paper is available at [###](#).

623 Reprints and permissions information is available at www.nature.com/reprints.

624 Correspondence and requests for materials should be addressed to Florian Ricour.

625 The codes for the data analysis were developed by F. Ricour. They were uploaded on GitHub
626 (at XXX) and are also available in the Zenodo repository (XXX).

627 Publisher’s note: Springer Nature remains neutral with regard to jurisdictional claims in
628 published maps and institutional affiliations.